bioRxiv preprint first posted online Jun. 27, 2017; doi: http://dx.doi.org/10.1101/155002. The copyright holder for this preprint (which was not peer-reviewed) is the author/funder, who has granted bioRxiv a license to display the preprint in perpetuity. It is made available under a CC-BY-NC-ND 4.0 International license.

Melanism patches up the defective cuticular morphological traits through promoting the up-regulation of cuticular protein-coding genes in *Bombyx mori*

Liang Qiao[*1], Ri-xin Wang[§], You-jin Hao[*], Hai Hu[§], Gao Xiong[§], Song-zhen He[§], Jiang-bo Song[§], Kun-peng Lu[§], Ya-qun Xin[†], James Mallet[‡], Bin Chen[*], Fang-yin Dai[§1]

***** Chongqing Key Laboratory of Vector Insects, Institute of Entomology and Molecular Biology, College of Life Sciences, Chongqing Normal University, Chongqing, 401331, China

[§] State Key Laboratory of Silkworm Genome Biology; Key Laboratory of Sericultural Biology and Genetic Breeding, Ministry of Agriculture; College of Biotechnology, Southwest University, Chongqing 400716, China.

† Department of Evolutionary Ecology, LMU Munich Großhaderner Str. 2, 82152, Germany

‡ Department of Organismic and Evolutionary Biology, Harvard University, Cambridge, MA 02138, USA

bioRxiv preprint first posted online Jun. 27, 2017; doi: http://dx.doi.org/10.1101/155002. The copyright holder for this preprint (which was not peer-reviewed) is the author/funder, who has granted bioRxiv a license to display the preprint in perpetuity. It is made available under a CC-BY-NC-ND 4.0 International license.

Running title: Role of melanin on cuticle defects

Keywords: Melanic coloring; Cuticle features; Cuticular protein-encoding genes; Induction; *Bombyx mori*

[1] **Corresponding Authors:**

Liang Qiao, Chongqing Key Laboratory of Vector Insects, Institute of Entomology and Molecular Biology, College of Life Sciences, Chongqing Normal University, No. 37 Daxuecheng Road, Chongqing, 401331, China; E-mail: qiaoliangswu@163.com; Tel: 86-23-65910315

Fang-yin Dai, State Key Laboratory of Silkworm Genome Biology, Key Laboratory for Sericulture Functional Genomics and Biotechnology of Agricultural Ministry, Southwest University, No. 2 Tiansheng Road, Chongqing, +86-23-68400715, China; E-mail: fydai@swu.edu.cn; Tel: 86-23-68250346

bioRxiv preprint first posted online Jun. 27, 2017; doi: http://dx.doi.org/10.1101/155002. The copyright holder for this preprint (which was not peer-reviewed) is the author/funder, who has granted bioRxiv a license to display the preprint in perpetuity. It is made available under a CC-BY-NC-ND 4.0 International license.

Abstract

Melanin and cuticular proteins are important cuticle components in insect. Cuticle defects caused by mutations in cuticular protein-encoding genes can hinder melanin deposition. However, the effects of melanin variation on cuticular protein-encoding genes and the corresponding morphological traits associated with these genes are remain largely unknown. Using *Bombyx mori* as a model, we showed that the melanism levels during larval cuticle pigmentation correlated positively with the expression of cuticular protein-encoding genes. This correlation stemmed from the simultaneous induction of these genes by the melanin precursors. More importantly, the effect of the melanism background on the cuticles induced the up-regulation of other functionally redundant cuticular protein-encoding genes to rescue the morphological and adaptive defects caused by the dysfunction of some mutated cuticular proteins, and the restorative ability increased with increasing melanism levels, which gives a novel evidence that melanism enhances insect adaptability. These findings deepen our understanding of the interactions among cuticle components, as well as their importance in the stabilizing of the normal morphology and function of the cuticle.

Introduction

The prerequisite for the benefits of melanism to insect is not only the integrity of the melanin biosynthesis and regulatory pathway (Wilson *et al.* 2001; Liu *et al.* 2015; Mallet and Hoekstra 2016), but also the normal presence of the platform it relied on

bioRxiv preprint first posted online Jun. 27, 2017; doi: http://dx.doi.org/10.1101/155002. The copyright holder for this preprint (which was not peer-reviewed) is the author/funder, who has granted bioRxiv a license to display the preprint in perpetuity. It is made available under a CC-BY-NC-ND 4.0 International license.

(Wittkopp *et al.* 2003; Wittkopp and Beldade 2009; Andersen 2010; Moussian 2010; Van Belleghem *et al.* 2017). For the insects, the most important fundamental platform for the color pattern drawing is the cuticle (Hopkins and Kramer 1992; Andersen 2010; Moussian 2010). During shaping the cuticle, the maintenance and stability of the cuticle features depends on normal functional cuticular proteins and the interactions with other components (such as chitin) (Hopkins and Kramer 1992; Guan *et al.* 2006; Suderman *et al.* 2006; Andersen 2010; Moussian 2010; Chaudhari *et al.* 2011; Noh *et al.* 2016). Due to the crucial roles of cuticular proteins on cuticle development, when their coding genes are loss of function, the abnormal or defective cuticle will likely affect the deposition and attachment of melanin, which is not conducive to the performance of color pattern (Kanekatsu *et al.* 1988; Oota and Kanekatsu 1993; Arakane *et al.* 2012; Jasrapuria *et al.* 2012; Wang 2013; Noh *et al.* 2015). Yet little is known about the corresponding response mode of cuticular protein-encoding genes via the alteration of the melanin biosynthesis or regulatory pathway.

Recently, several high throughput expression surveys showed that the abundance of cuticular protein-encoding genes in different colored integuments varied in some insect species, especially with evidently up-regulated in the melanic regions (Futahashi *et al.* 2012; He *et al.* 2016; Wu *et al.* 2016; Tajiri 2017), and some of those shared very similar expression patterns and functions (Nakato *et al.* 1994; Nakato *et al.* 1997; Shofuda *et al.* 1999; Okamoto *et al.* 2008; Liang *et al.* 2010; Tang *et al.* 2010; Qiao *et al.* 2014).These studies implied that there are probably some relationships between the promotion of melanism and the expression of cuticular

bioRxiv preprint first posted online Jun. 27, 2017; doi: http://dx.doi.org/10.1101/155002. The copyright holder for this preprint (which was not peer-reviewed) is the author/funder, who has granted bioRxiv a license to display the preprint in perpetuity. It is made available under a CC-BY-NC-ND 4.0 International license.

89 protein-encoding genes. Prior to this study, further exploring and understanding of the
90 potential relationships were unclear. Additionally, when melanism-promoting
91 instructions and defective cuticle proteins occur simultaneously, what are the effects
92 of their relationships on the presence of the corresponding morphological traits ?

93 In the Lepidoptera model, *Bombyx mori*, an intriguing phenomenon has been
94 reported that a larval melanic mutant, *Striped* (p^S, 2-0.0) is able to rehabilitate the
95 malformed body shape, as well as the adaptability defects of the *stony* mutant (*st*,
96 8-0.0) (Xiang 1995; Banno *et al.* 2005). A recent study clarified that a transcription
97 factor, *Apontic-like*, which boosts the expression of melanin synthesis genes in
98 epidermal cells, is responsible for the p^S mutant (Yoda *et al.* 2014). Besides this, there
99 are also multiple alleles with different melanism degrees at the *p* locus, including p^B,
100 p^M, *etc* (Xiang 1995; Banno *et al.* 2005; Yoda *et al.* 2014). And the *stony* mutant (*st*,
101 8-0.0) which precisely caused by the deletion of a RR1-type larval cuticular
102 protein-encoding gene, *BmLcp17* (or *BmorCPR2*) showed hard and tight touch feeling,
103 uncoordinated ratios of the length of the internodes and the intersegment folds (I/IF),
104 bulges at intersegment folds, and severely defective locomotion and behavioral
105 activities in the larval stage (Qiao *et al.* 2014). In addition, the similarity of the gene
106 expression patterns and functional characteristics among some members of the
107 RR1-type larval cuticular protein-encoding gene family, such as *BmLcp18*, *BmLcp22*,
108 *BmLcp30* also suggest that they may play very similar roles as *BmLcp17* in shaping
109 the larvae cuticle (Nakato *et al.* 1994; Nakato *et al.* 1997; Shofuda *et al.* 1999;
110 Okamoto *et al.* 2008; Liang *et al.* 2010; Tang *et al.* 2010; Qiao *et al.* 2014). These

bioRxiv preprint first posted online Jun. 27, 2017; doi: http://dx.doi.org/10.1101/155002. The copyright holder for this preprint (which was not peer-reviewed) is the author/funder, who has granted bioRxiv a license to display the preprint in perpetuity. It is made available under a CC-BY-NC-ND 4.0 International license.

111 dispersed findings are linked through the epistasis of p^S to *stony*, then provide the
112 breakthrough and the exceptional genetic resources for exploring the interactions
113 between melanin and cuticular protein-encoding genes.

114 Here we illustrated that the transcripts levels of four cuticular protein-encoding
115 genes were positively correlated with the melanism degree of larval cuticle, which
116 were due to the simultaneous induction these genes by the intracellular melanin
117 precursors. Moreover, by importing melanism-promoting instruction into the *stony*
118 mutant, the cuticle deficiency rescued through functionally redundant compensation
119 by some other up-regulated cuticular protein-encoding genes, which a new evidence
120 that melanism as a beneficial trait. These findings deepen our understanding of the
121 interactions among genetic factors which shape morphological features in
122 lepidopteran, and emphasize the ecological and evolutionary significance of these
123 mutual interactions.

124

125 **Materials and Methods**

126 ***Silkworm strains***

127 Wild-type strains Dazao ($+^p$) and melanic mutant strains p^M, p^S and p^B (Xiang 1995;
128 Banno *et al.* 2005; Yoda *et al.* 2014) were analyzed in this study. The darkness of
129 pigment was measured as mean OD value using Image J (https://imagej.nih.gov/ij/).
130 In terms of melanism degree, the body color of an individual that is homozygous at
131 one of the aforementioned melanic loci is darker than that of a heterozygous
132 individual (Xiang 1995; Banno *et al.* 2005). The albinism mutant *albino* (*al*) (Banno

bioRxiv preprint first posted online Jun. 27, 2017; doi: http://dx.doi.org/10.1101/155002. The copyright holder for this preprint (which was not peer-reviewed) is the author/funder, who has granted bioRxiv a license to display the preprint in perpetuity. It is made available under a CC-BY-NC-ND 4.0 International license.

133 *et al.* 2005; Fujii *et al.* 2013), non-diapause wild-type strain N4 (used for melanin
134 inhibition treatment) and *BmLcp17* deletion strain Dazao-*stony* (near isogeneic line of
135 Dazao, which have been backcrossed with Dazao over 26 generations) were supplied
136 by the Silkworm Gene Bank in Southwest University. The N4 strain and *al* mutant
137 were fed with artificial diet at 28℃, and the others were fed fresh mulberry leaves
138 under a 12□h/12□h light/dark photoperiod at 24□℃.

139 ***Chemicals and cell lines***

140 L-dopa (D9628), dopamine (H8502), tetrahydrofolic acid (BH_4) (T3125) and
141 2,4-Diamino-6-hydroxypyrimidine (DAHP) (D19206) were purchased from
142 Sigma-Aldrich (St. Louis, MO, USA). *BmNs* cell line was kept in our laboratory.

143 ***Mating combinations and progeny phenotypes identification***

144 The p^S and p^M strains were crossed with the Dazao-*stony* strain to generate the F_1
145 generation, respectively. The F_2 generation were produced by an F_1 self-cross, and
146 individuals of day 5 of the fifth-instar were collected to further use. The p^B strain was
147 crossed with the Dazao-*stony* strain to generate F_1 progeny, which mated with the
148 Dazao-*stony* strain to generate the BC_1 generation, and fed them until at day 5 of the
149 fifth-instar. Firstly, individuals of the F_2 or BC_1 generations were separated by their
150 cuticle pigmentation. Subsequently, their phenotypes were further classified by
151 morphological characteristics, touch feeling, and the ratios between the number of
152 internodes and intersegmental folds in the second, third, and fourth abdominal
153 segments based on an earlier method (Qiao *et al*. 2014).

154 ***Genotyping***

bioRxiv preprint first posted online Jun. 27, 2017; doi: http://dx.doi.org/10.1101/155002. The copyright holder for this preprint (which was not peer-reviewed) is the author/funder, who has granted bioRxiv a license to display the preprint in perpetuity. It is made available under a CC-BY-NC-ND 4.0 International license.

Because the p^S, p^M and p^B mutations are alleles at the *p* locus, they should be located in proximity each other on the chromosome 2 (Xiang 1995; Banno *et al*. 2005; Yoda *et al.* 2014). Based on the reported sequence of the gene corresponding to the p^S allele, a polymerase chain reaction (PCR)-based molecular marker within of the genomic region of the *Apontic-like* was designed. PCR screening were performed in the p^X (*X*=*M*, *S* and *B*) and Dazao-*stony* to obtain the polymorphism molecular marker for *p* locus. Similarly, molecular marker was also designed within genomic region of the *BmLcp17* for polymorphism screening of the *stony* locus. The primers used in this study are listed in Table S1.

Association analysis of gene expression, phenotype and genotype

Day 5 fifth-instar larvae of the Dazao or Dazao-*stony* strains were selected for cuticle dissection. The cuticles of the semi-lunar marking region and the non-melanic portion between the paired semi-lunar marking were finely dissected. Gene expression levels of *BmLcp17*, *BmLcp18*, *BmLcp22* and *BmLcp30* in these regions were compared. Gene expression patterns were determined for the dorsal epidermis of abdominal segments (from semi-lunar marking to star marking) from day 5 of fifth instar larvae (Dazao, p^S/+, p^M/+, p^B/+). Day 1 of second instar larvae of the *al* and Dazao strains were also investigated. The same regions of dorsal epidermis regions were collected from F_2-generation individuals with the p^S/p^S, *st/*st, and p^S/+, *st/st* genotypes, as well as the p^M/p^M, *st/st* and p^M/+, *st/st* genotypes for gene expression analyses. For all genotyped individuals, the ratios of the intersegment length to the intersegment fold were also analysed using image J.

bioRxiv preprint first posted online Jun. 27, 2017; doi: http://dx.doi.org/10.1101/155002. The copyright holder for this preprint (which was not peer-reviewed) is the author/funder, who has granted bioRxiv a license to display the preprint in perpetuity. It is made available under a CC-BY-NC-ND 4.0 International license.

177 ***Melanin precursors-promoting and inhibition treatments***

178 The preparation and concentration of L-dopa and dopamine solutions were slightly
179 modified according to the description by Futahashi (Futahashi and Fujiwara 2005),
180 and filtered with a 0.22 μm membranes before use. Cells were washed three times
181 with Grace medium without melanin precursors to remove metabolites and other
182 contaminants on the cell surfaces. Medium (0.8 mL) containing L-dopa or dopamine
183 was added separately into each well, and the medium without melanin precursors was
184 used as the control. Culture plates were sealed with tape, wrapped with foil and
185 incubated at 28℃ for 24 h for a gene expression analysis. For BH_4 feeding assays,
186 the 30mM working solution was prepared by dissolving tetrahydrofolic acid into
187 ddH_2O, and spreading it on an artificial diet for *al* mutants. The control was ddH_2O.
188 Phenotype were observed and recorded from the second instar stage, and expression
189 of cuticular protein-encoding genes was analysed. For the melanism-inhibition
190 experiments, the wild-type strain N4 was used. Newly-hatched larvae were divided
191 into treatment and control groups. Individuals in the treatment group fed with DAHP
192 dissolved in 0.1M NaOH (15g/L), and individuals in the control group fed 0.1M with
193 NaOH. Phenotypes observation and gene expressions detection were performed on
194 day 1 of the second-instar larvae.

195 ***Quantitative RT–PCR***

196 Total RNA extraction, reverse transcription and Quantitative reverse
197 transcription-PCR (qRT-PCR) conducted as described previously (Qiao *et al.* 2014).
198 Three biological replicates were prepared for each condition, and *BmRPL3* was used

bioRxiv preprint first posted online Jun. 27, 2017; doi: http://dx.doi.org/10.1101/155002. The copyright holder for this preprint (which was not peer-reviewed) is the author/funder, who has granted bioRxiv a license to display the preprint in perpetuity. It is made available under a CC-BY-NC-ND 4.0 International license.

as the internal control. Primers are listed in Table S1.

Results

Entirely distinct expression patterns of cuticular protein-encoding genes and the cuticle appearance between melanic and non-melanic regions

Expression patterns of *BmLcp17*, *BmLcp18*, *BmLcp22* and *BmLcp30* in melanic or non-melanic epidermal regions are shown in Figure 1. These results, together with earlier studies (Futahashi *et al.* 2012; He *et al.* 2016; Wu *et al.* 2016), revealed that the gene expressions were significantly higher in melanic parts of the cuticle than in non-melanic parts. Moreover, micro protrusions were more intensive in the melanic regions than in the non-melanic regions, and accompanied by a higher amounts of chitin (another important cuticle component (Hopkins and Kramer 1992; Moussian *et al.* 2006; Andersen 2010; Moussian 2010; Chaudhari *et al.* 2011; Qiao *et al.* 2014), and the reduction chitin content was reported to impede cuticle melanism (Moussian *et al.* 2005)) (Figure S1A). These results showed that, regardless of the different genetic basis of the melanic mutants or the melanic markings in the non-melanic strains, excessive accumulation of melanin in the cuticle (accompany by the changes in the surface structure and the chitin content of the melanic cuticle) was closely related to the high expression levels of the cuticular protein-encoding genes.

Expression level of larval cuticular protein-encoding genes positively correlated with the degree of cuticle melanism

To obtain further insights into the relationships between the melanin accumulation

bioRxiv preprint first posted online Jun. 27, 2017; doi: http://dx.doi.org/10.1101/155002. The copyright holder for this preprint (which was not peer-reviewed) is the author/funder, who has granted bioRxiv a license to display the preprint in perpetuity. It is made available under a CC-BY-NC-ND 4.0 International license.

and the expression of cuticular protein-encoding genes, we investigated gene expression patterns using four *p* locus alleles (Dazao ($+^{p}$), p^{M}, p^{S} and p^{B}), which showed gradually increasing melanin accumulation (Figure 2A). Gene expression levels were gradually and significantly up-regulated with the increase in the degree of melanism in cuticle (Figure 2B). These results further showed that the expression levels correlated positively with the degree of melanism. Thus, the quantities of cuticular proteins with similar or redundant functions was increased greatly by the increasing the degree of melanism.

Typical stony phenotyped individuals masked after the introduction of melanic loci into the BmLcp17 defection strain

We assessed the effects of modulating the melanic background on the phenotypic defects caused by the deletion of *BmLcp17*. After mating the p^{B} and *stony* parental, the percentage of BC_1 individuals with melanism and the normal body shape in the backcrossed population of the p^{B}×*stony* cross was 52 % (290/553; and theoretically, it was 25 %), yet individuals with the melanism cuticle and *stony*-type body shape were not found (theoretically should be almost equivalent to the number of individuals with melanism cuticle and normal body shape) (Figure 3). In the cross of p^{S}×*stony*, ~10.8% (36/331) of F_2 progeny had an lighter melanism body color and smaller body size (Figure 3). These individuals exhibited a little hard and tight touched body, but the body was much softer than that of the *stony* mutant. Their intersegment folds bulged slightly, and the length were significantly shorter than that of the internodes; accordingly, their phenotypes slightly resembled the morphological features of the

bioRxiv preprint first posted online Jun. 27, 2017; doi: http://dx.doi.org/10.1101/155002. The copyright holder for this preprint (which was not peer-reviewed) is the author/funder, who has granted bioRxiv a license to display the preprint in perpetuity. It is made available under a CC-BY-NC-ND 4.0 International license.

243 *stony* mutant (Figure 3 and 4A). Even so, We did not find individuals with the typical
244 *stony*-type body shape and also defective adaptability under the melanism background
245 (theoretical ratio is 3/16). (Figure 3). Similarly, in the p^M×*stony* corss, only
246 approximately ~11.7% (51/437) of the individuals of the F_2 population were very
247 lightly melanic, but they exhibited obviously unusual morphological features (Figure
248 3, Figure 4A). When compared with the ~10.8% F_2 individuals (aforementioned) from
249 the p^S×*stony* cross, the touch feelings of individuals from the p^M×*stony* cross were
250 tighter and firmer, and the intersegment folds bulged more obviously and had a higher
251 proportion among the segments, meaning that their body features were closer to the
252 phenotype of the *stony* mutant (Figure 3 and 4A) (Qiao *et al.* 2014). Nevertheless,
253 melanic individuals showing the typical *stony*-type body features and defective
254 adaptability still did not appear (theoretical ratio is 3/16) in the progeny from the p^M ×
255 *stony* cross. Therefore, induction of the melanic mutation into individuals with a
256 defective cuticular protein-encoding gene could mask the adverse phenotypes, and the
257 masking effect was more remarkable with the increasing degree of melanism.

258 ***Other larval cuticular protein-encoding genes up-regulated evidently in the melanic***
259 ***and non-stony phenotypic, but with mutated BmLcp17 genotypic offspring***

260 Using the molecular markers (closely linked to the *p* and *st* loci, respectively), we
261 further genotyped the progenies with melanic color pattern and non-*stony* (including
262 ambiguous *stony*-like) body shape. The results revealed that approximately 49% of
263 the individuals showing a melanic color and normal body shape in the BC_1 population
264 from the p^B×*stony* cross was the $p^B/+^{pB}$, *st/st* genotype (Figure 4A). The ratios of the

bioRxiv preprint first posted online Jun. 27, 2017; doi: http://dx.doi.org/10.1101/155002. The copyright holder for this preprint (which was not peer-reviewed) is the author/funder, who has granted bioRxiv a license to display the preprint in perpetuity. It is made available under a CC-BY-NC-ND 4.0 International license.

length of the internodes and the intersegment folds (I/IF) were ~4, which is very similar to that in $p^{B}/+^{pB}$, $+^{st}/st$ individuals, and also no significant differences as that in the wild-type individuals (Figure 4B) (Qiao *et al*. 2014). In the F_2 generation from the p^{S}×*stony* cross, approximately 9.3% of the individuals with the p^{S}/p^{S}, *st*/*st* genotype and very few individuals (~1%) with the genotype $p^{S}/+^{pS}$, *st/st* exhibited a melanic color and the normal body shape (Figure 4A). For p^{S}/p^{S}, *st/st* genotyped individuals, the I/IF value was approximately 3.3 (Figure 4B). Although the I/IF value was lower than that in $p^{S}/_$, $+^{st}/_$ individuals (approximately 4, Figure 4B), it was much higher than that in the *stony* mutant (approximately 1.6 (Qiao *et al*. 2014)). Despite the slightly smaller body size of the p^{S}/p^{S}, *st/st* individuals, their body shape was essentially normal (Figure 4A). The genotypes of those lightly melanic individuals, whose body shape was slightly like that of the *stony* phenotype (mentioned in Result 3), were all the $p^{S}/+^{pS}$, *st*/*st*, and the I/IF value of these individuals was approximately 2.7 (Figures 4A and 4B). In progeny of the p^{M}×*stony* cross, ~10.5% of the individuals with the p^{M}/p^{M}, *st/st* genotype and ~0.7 % of the individuals with the $p^{M}/+^{pM}$, *st/st* genotype showed a melanic color and subtle *stony* features (just very slight bulges) (Figure 4A). The body size of the p^{M}/p^{M}, *st/st* individuals were smaller than those of the $p^{M}/_$, $+^{st}/_$ individuals. They exhibited a certain sense of hardness, and the I/IF ratio was approximately 2.8, which is in good agreement with their phenotypes (Figure 4B). Additionally, individuals showing very slight melanism and morphological features that were more similar to that of the *stony* mutant (mentioned in Result 3) were all the $p^{M}/+^{pM}$, *st/st* genotype, and their I/IF values were

bioRxiv preprint first posted online Jun. 27, 2017; doi: http://dx.doi.org/10.1101/155002. The copyright holder for this preprint (which was not peer-reviewed) is the author/funder, who has granted bioRxiv a license to display the preprint in perpetuity. It is made available under a CC-BY-NC-ND 4.0 International license.

287 approximately 1.8, which is closer to that of the *stony* mutant (Figures 4A and 4B). In
288 addition, the expression of cuticular protein-encoding genes in p^{S}/p^{S}, *st/st* individuals
289 were significantly higher than that in $p^{S}/+^{pS}$, *st/st* individuals (Figure. 4C); a similar
290 result was also obtained from the p^{M}/p^{M}, *st/st* and $p^{M}/+^{pM}$, *st/st* individuals (Figure 4C).
291 Taken together, these results revealed that more cuticular proteins with similar
292 functions were accumulated in the cuticle of melanic homologous individuals at the *p*
293 locus. Based on the comprehensive and association analysis, we infer that melanic
294 background effectively drove the expressions of cuticular protein-encoding genes
295 with similar expression patterns and redundant functions, which compensated for the
296 morphological and adaptability defects caused by the dysfunctional *BmLcp17* gene;
297 and the law of compensatory abilities was $p^{B}/+^{pB}$, *st/st* > p^{S}/p^{S}, *st/st* > p^{M}/p^{M}, *st/st* ≮
298 $p^{S}/+^{pS}$, *st/st* > $p^{M}/+^{pM}$, *st/st*, which corresponds well with the gradual weakening of the
299 degree of melanism (Figures 4 and Figure S3).

300 ***Content variations of melanin precursors affect the transcript amount of the***
301 ***cuticular protein-encoding genes***

302 Due to the crucial material basis for the cuticle melanism (no matter what kind of
303 genetic basis caused by) is the extensive accumulation of melanin precursors in the
304 epidermal cells; thus, the essence that melanism tend to increase the expression of
305 some cuticular protein-encoding genes should be driven by the relations between the
306 accumulation of melanin precursors and the transcripts amount of the cuticular
307 protein-encoding genes. The basal expressions of four cuticular protein-encoding
308 genes were detected in *BmNs* cells (Figure S5) and indicated that regulatory pathways

bioRxiv preprint first posted online Jun. 27, 2017; doi: http://dx.doi.org/10.1101/155002. The copyright holder for this preprint (which was not peer-reviewed) is the author/funder, who has granted bioRxiv a license to display the preprint in perpetuity. It is made available under a CC-BY-NC-ND 4.0 International license.

controlling the expression of cuticular protein-coding genes in this cell line. Thus, this cell line was used to examine the effect of melanin precursors on gene expressions. After incubating *BmNs* cells with melanin precursors, the expression of cuticular protein-encoding genes was significantly higher in cells treated either by L-dopa or dopamine, compare with that in the control group (Figure 5 top (left)). Second-instar *al* mutant are characterized by albinism and a porous cuticle due to a mutation in sepiapterin reductase, which leads to the insufficient synthesis of the co-factor BH_4 during the synthesis of melanin precursors (Banno *et al.* 2005; Fujii *et al.* 2013). When treated with BH_4, these mutants had normal melanic body color (Lab unpublished contribution) (Fujii *et al.* 2013), and gene expressions were obviously higher than that in the control group (Figure 5 top (right)). These results suggested that the expression of cuticular protein-encoding genes was induced by increasing amounts of melanin precursors. We investigated the effects of DAHP, an inhibitor of guanylate cyclase hydrolase (GTPCHI), an important rate-limiting enzyme in the synthesis of BH_4 (Hamadate *et al.* 2008). Inhibiting BH_4 synthesis in wild-type second-instar larvae by blocking the synthesis of melanin precursors in epidermal cells caused individuals to lose their original melanic body color (Lab unpublished contribution). The gene expressions were also significantly reduced when compared with that in the control group (Figure 5 bottom). Thus, the content and variation of the intracellular melanin precursors were important factors for regulating the expression of cuticular protein-encoding genes. We concluded that the inducing effect of the melanin precursors on the expression of cuticular protein-encoding genes is the basis

bioRxiv preprint first posted online Jun. 27, 2017; doi: http://dx.doi.org/10.1101/155002. The copyright holder for this preprint (which was not peer-reviewed) is the author/funder, who has granted bioRxiv a license to display the preprint in perpetuity. It is made available under a CC-BY-NC-ND 4.0 International license.

for melanism promoting genes‘ transcription.

Discussion

Melanin is mainly deposited in the epicuticle and exocuticle, cross-linked with proteins in this layer, and involved in the formation of the melanic cuticular characteristics (Hopkins and Kramer 1992; Suderman *et al.* 2006; Andersen 2010; Moussian 2010; Hu *et al.* 2013). Some cuticular proteins located in the endocuticle may not be directly associated with the melanin, but the maintaining of the normal cuticle need to rely on the normal development and coordination between each cuticle layer, and these proteins are indispensable element in shaping the endocuticle (Moussian 2010; Cohen and Moussian 2016). Thus, we suppose that these endocuticular proteins may influence the transportation or accumulation of melanin through some indirect ways, to contribute to the unique features of the melanic cuticle. We indeed clearly observed that extensive star-like protrusions were present on the cuticle when a large amount of melanin accumulated (Figure S1). Similar correlations between cuticle structure and body color have been reported multiple times (Futahashi *et al.* 2012; Noh *et al.* 2016; Tan *et al.* 2016), imply that there should be some interactions between cuticular proteins and melanin. Although the exact interaction pattern between these two cuticular components is unknown, microscopic observation clearly shows that the deposition of an excessive amount of melanin affected the cuticle characteristics.

The expression profile of cuticular protein-encoding genes in melanic silkworm

bioRxiv preprint first posted online Jun. 27, 2017; doi: http://dx.doi.org/10.1101/155002. The copyright holder for this preprint (which was not peer-reviewed) is the author/funder, who has granted bioRxiv a license to display the preprint in perpetuity. It is made available under a CC-BY-NC-ND 4.0 International license.

353 mutants and the black markings of *Papilio* larvae supported the hypothesis that
354 up-regulated cuticular proteins probably participate in the transport or maintenance of
355 the corresponding pigments in a specifically colored cuticles (Figures 1, 2 and Figure
356 S1) (Futahashi *et al.* 2012; He *et al.* 2016; Wu *et al.* 2016). Yet over-expression of
357 cuticular protein-encoding genes *in vivo* cannot trigger (or induce) the formation of
358 melanic cuticle (Tajiri *et al.* 2017). Therefore, we hypothesized that if instructions for
359 melanin accumulation were included in the developmental program for which
360 melanism is the original factor, other cuticle features and structures would adapt to the
361 level of melanin accumulation, regardless of genetic background. The up-regulation
362 of cuticular protein-encoding genes should be a necessary adaptation for the
363 maintenance and stability of the structural characteristics and physical properties of
364 melanic cuticles. The relationship of melanin and cuticular proteins at the
365 ultrastructural level deserves special attention in follow-up studies.

366 Although the elaborate regulatory mechanism by which melanin precursors affect
367 the expression of cuticular protein-encoding genes is unclear, our results revealed the
368 existence of this regulatory phenomenon (Figure 5). Cuticle formation is regulated
369 stringently by temporal and spatial patterns, the accumulation and oxidization of
370 melanin precursors, and interactions such as crosslinking among other components
371 should occur after the initial cuticle formation (Moussian 2010; Sobala and Adler
372 2016; Tajiri 2017). Therefore, we propose that the cuticular proteins induced by
373 melanin precursors are used to create a platform for further shaping and perfection of
374 the melanic cuticle. When melanin-associated protein-encoding genes have similar

bioRxiv preprint first posted online Jun. 27, 2017; doi: http://dx.doi.org/10.1101/155002. The copyright holder for this preprint (which was not peer-reviewed) is the author/funder, who has granted bioRxiv a license to display the preprint in perpetuity. It is made available under a CC-BY-NC-ND 4.0 International license.

375 expression patterns and functions (Nakato *et al.* 1994; Nakato *et al.* 1997; Shofuda *et*
376 *al.* 1999; Okamoto *et al.* 2008; Liang *et al.* 2010; Tang *et al.* 2010; Qiao *et al.* 2014),
377 the production of large amounts of functionally similar cuticular proteins would be
378 driven by the melanic background to guarantee construction and stability of the
379 melanic cuticle. During this process, melanism would unlocks the complementary
380 features of melanin-associated cuticular proteins (such as *BmLcp18*, *BmLcp22*,
381 *BmLcp30*), rescued cuticular malformation caused by the loss of function of some
382 cuticular proteins (such as defected *BmLcp17* in *stony* mutant). Because a special
383 cuticle-forming pattern appears to be regulated by melanin accumulation, melanism
384 may enhance insect adaptability to avoid the impairment of survival caused by
385 mutations and/or functional loss of some cuticular proteins, and our results also add
386 new evidence to explain how melanism can be a beneficial trait (Wilson *et al.* 2001;
387 True 2003; Wittkopp *et al.* 2003; Wittkopp and Beldade 2009; Liu *et al.* 2015; Mallet
388 and Hoekstra 2016).

389 As far as we known, there is no evidence to suggest that the four larval cuticular
390 proteins (as structure proteins) and their orthologous can enter the nucleus and
391 regulate gene expression by acting as transcription factors. In addition, our findings
392 and some other studies showed that changes in the expression of one cuticular
393 protein-encoding genes of R&R family did not affect the expression of other members
394 (Figure S6, S7) (Arakane *et al.* 2012; Noh *et al.* 2015). Moreover, several studies
395 reveal that organisms optimize resources allocation at gene or protein expression level
396 (Liebermeister *et al.* 2004; Dekel and Alon 2005), and there is no report that the

bioRxiv preprint first posted online Jun. 27, 2017; doi: http://dx.doi.org/10.1101/155002. The copyright holder for this preprint (which was not peer-reviewed) is the author/funder, who has granted bioRxiv a license to display the preprint in perpetuity. It is made available under a CC-BY-NC-ND 4.0 International license.

397 cuticular proteins have long range morphogen effects (such as wingless) to regulate
398 their encoding genes by feedback regulation from the cuticle to the epidermal cells;
399 thus, the expression of melanin associated cuticle protein-encoding genes should be
400 appropriately and simultaneously coordinated with the sufficient accumulation of
401 intracellular melanin precursors, as a relatively direct, economical, efficient and
402 convenient strategy. Furthermore, DAHP inhibits GTPCHI activity, but it does not
403 directly impair the extracellular accumulation of melanin and protein–protein
404 interactions in the cuticle. Finally, there is some evidence that melanin precursors
405 regulate gene expressions via the receptors (Konradi *et al.* 1996; Berke *et al.* 1998;
406 Westin *et al.* 2001). In summary, we hypothesized that the up-regulation of the four
407 *BmLcp* genes were induced simultaneously by excessive amounts of melanin
408 precursors, but should not be the interaction among these four genes on regulation
409 level. To test our hypothesis, further analyses will be performed to determine the
410 expression of the remaining *BmLcp* genes in some *BmLcps* mutant (such as defective
411 *BmLcp17*) cell line by increasing or decreasing the melanin precursors content.

412 The markings were lighter in the *stony* mutant than in the wild-type strain, and
413 were accompanied by the downregulation of melanin synthase genes (Figure S4). If
414 the dysfunction of some cuticular proteins cannot be effectively supplemented,
415 abnormalities of the cuticle structure and interactions of various cuticular components
416 may occur, probably resulting in barriers to melanin deposition and metabolism. This
417 dysfunction might be the reason why the $p^{S}/+^{pS}$, *st/st* (or $p^{M}/+^{pM}$, *st/st*) genotypes was
418 lighter than the $p^{S}/+^{pS}$, $+^{st}/_$ (or $p^{M}/+^{pM}$, $+^{st}/_$) genotypes and had a different body

bioRxiv preprint first posted online Jun. 27, 2017; doi: http://dx.doi.org/10.1101/155002. The copyright holder for this preprint (which was not peer-reviewed) is the author/funder, who has granted bioRxiv a license to display the preprint in perpetuity. It is made available under a CC-BY-NC-ND 4.0 International license.

shape. Because the homozygous of p^B mutation is lethal (Xiang 1995; Banno *et al.* 2005), we were unable to obtain F_2 progeny with the p^B/p^B, *st/st* genotype. However, we note that the $p^B/+^{pB}$, $+^{st}/st$ and $p^B/+^{pB}$, *st/st* genotype individuals had almost the same body shape and melasnism (Figure 4A). Therefore, we propose that during cuticle formation, if the signal promoting melanism is sufficiently strong, sufficient melanin precursors should be generated. The contents of functionally redundant proteins induced by melanin precursors are sufficient to fill the gap generated by the dysfunction of some cuticular proteins, guaranteeing the normal accumulation of melanin. Therefore, we hypothesize a threshold for the melanism-promoting effect. When the accumulation of melanin precursors spans this threshold, the requirements for cuticular proteins with similar function are not lowered, even when one of them loses the function. This effect would guarantee the formation of a normal cuticle structure, ensuring subsequent pigmentation.

We propose the following regulatory model: when large amounts of melanin precursors induced by endogenous- and/or exogenous melanism-promoting factors, it may directly or indirectly induce the up-regulation of some cuticular protein-encoding genes. This upregulation guarantees the formation of normal structural features of the melanic cuticle. During this process, if some cuticular proteins lose function, other functionally redundant cuticular proteins induced by melanin precursors compensate for the functional defects. Compensatory intensity increases with increasing melanin accumulation. When melanin accumulation spans a certain threshold, compensation completely masks the defective phenotype caused by the malfunctioning genes. This

bioRxiv preprint first posted online Jun. 27, 2017; doi: http://dx.doi.org/10.1101/155002. The copyright holder for this preprint (which was not peer-reviewed) is the author/funder, who has granted bioRxiv a license to display the preprint in perpetuity. It is made available under a CC-BY-NC-ND 4.0 International license.

model adds to growing evidence that melanism may have pleiotropic effects that enhance adaptability over and above the effect of melanin accumulation itself (Figure 6). Due to the coexistence of excess melanin and cuticular proteins is common in other insects, and homologues the four *BmLcp* gene are widely distributed in the Lepidoptera (Table S2), we presume that the above reciprocal action and its corresponding biological significance are conserved in other Lepidoptera insects to that in *Bombyx mori*.

In summary, we used crucial cuticle components to elucidate the mutual effects among some key genetic factors, and the physiological significance of these mutual effects during the development of the morphological features. Our findings contribute a realistic basis for in-depth study on the interaction patterns of melanin and cuticular proteins, and will also guide relevant studies in other Lepidopteran insects or other insect species.

Literature Cited

Andersen, S. O., 2010 Insect cuticular sclerotization: a review. Insect Biochem Mol Biol 40**:** 166-178.

Arakane, Y., J. Lomakin, S. H. Gehrke, Y. Hiromasa, J. M. Tomich *et al.*, 2012 Formation of rigid, non-flight forewings (elytra) of a beetle requires two major cuticular proteins. PLoS Genet 8**:** e1002682.

Banno, Y., H. Fujii, Y. Kawaguchi, K. Yamamoto, K. Nishikawa *et al.*, 2005 *A guide to the silkworm mutants: 2005 gene name and gene symbol*. Kyusyu University, Fukuoka, Japan.

Berke, J. D., R. F. Paletzki, G. J. Aronson, S. E. Hyman and C. R. Gerfen, 1998 A complex program of striatal gene expression induced by dopaminergic stimulation. J Neurosci 18**:** 5301-5310.

Chaudhari, S. S., Y. Arakane, C. A. Specht, B. Moussian, D. L. Boyle *et al.*, 2011 Knickkopf protein protects and organizes chitin in the newly synthesized insect exoskeleton. P Natl Acad Sci USA 108**:** 17028-17033.

Cohen, E., and B. Moussian, 2016 *Extracellular Composite Matrices in Arthropods*. Springer, Switzerland.

Dekel, E., and U. Alon, 2005 Optimality and evolutionary tuning of the expression level of a protein.

bioRxiv preprint first posted online Jun. 27, 2017; doi: http://dx.doi.org/10.1101/155002. The copyright holder for this preprint (which was not peer-reviewed) is the author/funder, who has granted bioRxiv a license to display the preprint in perpetuity. It is made available under a CC-BY-NC-ND 4.0 International license.

Nature 436: 588-592.

Fujii, T., H. Abe, M. Kawamoto, S. Katsuma, Y. Banno *et al.*, 2013 Albino (al) is a tetrahydrobiopterin (BH_4)-deficient mutant of the silkworm *Bombyx mori*. Insect Biochem Mol Biol 43: 594-600.

Futahashi, R., and H. Fujiwara, 2005 Melanin-synthesis enzymes coregulate stage-specific larval cuticular markings in the swallowtail butterfly, *Papilio xuthus*. Dev Genes Evol 215: 519-529.

Futahashi, R., H. Shirataki, T. Narita, K. Mita and H. Fujiwara, 2012 Comprehensive microarray-based analysis for stage-specific larval camouflage pattern-associated genes in the swallowtail butterfly, *Papilio xuthus*. BMC Biol 10: 46.

Guan, X., B. W. Middlebrooks, S. Alexander and S. A. Wasserman, 2006 Mutation of TweedleD, a member of an unconventional cuticle protein family, alters body shape in *Drosophila*. P Natl Acad Sci USA 103: 16794-16799.

Hamadate, N., K. Noguchi, M. Sakanashi, T. Matsuzaki, J. Nakasone *et al.*, 2008 Effect of decreased levels of intrinsic tetrahydrobiopterin on endothelial function in anesthetized rats. J Pharmacol Sci 107: 49-56.

He, S. Z., X. L. Tong, K. P. Lu, Y. R. Lu, J. W. Luo *et al.*, 2016 Comparative analysis of transcriptomes among *Bombyx mori* strains and sexes reveals the genes regulating melanic morph and the related phenotypes. Plos One 11.

Hopkins, T. L., and K. J. Kramer, 1992 Insect cuticle sclerotization. Annu Rev Entomol 37: 273-302.

Hu, Y. G., Y. H. Shen, Z. Zhang and G. Q. Shi, 2013 Melanin and urate act to prevent ultraviolet in the integument of the silkworm, *Bombyx mori*. Arch Insect Biochem 83: 41-55.

Jasrapuria, S., C. A. Specht, K. J. Kramer, R. W. Beeman and S. Muthukrishnan, 2012 Gene families of cuticular proteins analogous to peritrophins (CPAPs) in *Tribolium castaneum* have diverse functions. Plos One 7.

Kanekatsu, R., Y. Banno, E. Nagashima and T. Miyashita, 1988 Genetical studies on a new spontaneous mutant "*Bamboo*" (*Bo*) of the silkworm. The Journal of Sericultural Science of Japan 57: 151-156.

Konradi, C., J. C. Leveque and S. E. Hyman, 1996 Amphetamine and dopamine-induced immediate early gene expression in striatal neurons depends on postsynaptic NMDA receptors and calcium. J Neurosci 16: 4231-4239.

Liang, J., L. Zhang, Z. Xiang and N. He, 2010 Expression profile of cuticular genes of silkworm, *Bombyx mori*. BMC Genomics 11: 173.

Liebermeister, W., E. Klipp, S. Schuster and R. Heinrich, 2004 A theory of optimal differential gene expression. Biosystems 76: 261-278.

Liu, S. S., M. Wang and X. C. Li, 2015 Pupal melanization is associated with higher fitness in *Spodoptera exigua*. Sci Rep-Uk 5.

Mallet, J., and H. E. Hoekstra, 2016 Ecological genetics: a key gene for mimicry and melanism. Curr Biol 26: R802-R804.

Min, C., J. B. Song, L. I. Zhi-Quan, D. M. Tang, X. L. Tong *et al.*, 2016 Progress and perspective of silkworm as a model of human diseases for drug screening. Acta Pharmaceutica Sinica.

Moussian, B., 2010 Recent advances in understanding mechanisms of insect cuticle differentiation. Insect Biochem Mol Biol 40: 363-375.

Moussian, B., H. Schwarz, S. Bartoszewski and C. Nusslein-Volhard, 2005 Involvement of chitin in exoskeleton morphogenesis in *Drosophila melanogaster*. J Morphol 264: 117-130.

Moussian, B., E. Tang, A. Tonning, S. Helms, H. Schwarz *et al.*, 2006 *Drosophila* Knickkopf and

bioRxiv preprint first posted online Jun. 27, 2017; doi: http://dx.doi.org/10.1101/155002. The copyright holder for this preprint (which was not peer-reviewed) is the author/funder, who has granted bioRxiv a license to display the preprint in perpetuity. It is made available under a CC-BY-NC-ND 4.0 International license.

514 Retroactive are needed for epithelial tube growth and cuticle differentiation through their
515 specific requirement for chitin filament organization. Development 133**:** 163-171.
516 Nakato, H., K. Shofuda, S. Izumi and S. Tomino, 1994 Structure and developmental expression of a
517 larval cuticle protein gene of the silkworm, *Bombyx mori*. Biochim Biophys Acta 1218**:** 64-74.
518 Nakato, H., M. Takekoshi, T. Togawa, S. Izumi and S. Tomino, 1997 Purification and cDNA cloning of
519 evolutionally conserved larval cuticle proteins of the silkworm, *Bombyx mori*. Insect Biochem
520 Mol Biol 27**:** 701-709.
521 Noh, M. Y., S. Muthukrishnan, K. J. Kramer and Y. Arakane, 2015 *Tribolium castaneum* RR-1 cuticular
522 protein TcCPR4 is required for formation of pore canals in rigid cuticle. PLoS Genet 11.
523 Noh, M. Y., S. Muthukrishnan, K. J. Kramer and Y. Arakane, 2016 Cuticle formation and pigmentation
524 in beetles. Curr Opin Insect Sci 17**:** 1-9.
525 Okamoto, S., R. Futahashi, T. Kojima, K. Mita and H. Fujiwara, 2008 Catalogue of epidermal genes:
526 genes expressed in the epidermis during larval molt of the silkworm *Bombyx mori*. BMC
527 Genomics 9**:** 396.
528 Oota, K., and R. Kanekatsu, 1993 Morphological studies on the *Bamboo* (*Bo*) mutant of the silkworm,
529 *Bombyx mori*. The Journal of Sericultural Science of Japan 62**:** 448-454.
530 Qiao, L., G. Xiong, R. X. Wang, S. Z. He, J. Chen *et al.*, 2014 Mutation of a cuticular protein,
531 BmorCPR2, alters larval body shape and adaptability in silkworm, *Bombyx mori*. Genetics
532 196**:** 1103-1115.
533 Shofuda, K., T. Togawa, H. Nakato, S. Tomino and S. Izumi, 1999 Molecular cloning and
534 characterization of a cDNA encoding a larval cuticle protein of *Bombyx mori*. Comp Biochem
535 Physiol B Biochem Mol Biol 122**:** 105-109.
536 Sobala, L. F., and P. N. Adler, 2016 The gene expression program for the formation of wing cuticle in
537 *Drosophila*. PLoS Genet 12.
538 Suderman, R. J., N. T. Dittmer, M. R. Kanost and K. J. Kramer, 2006 Model reactions for insect cuticle
539 sclerotization: cross-linking of recombinant cuticular proteins upon their laccase-catalyzed
540 oxidative conjugation with catechols. Insect Biochem Mol Biol 36**:** 610-611.
541 Tajiri, R., 2017 Cuticle itself as a central and dynamic player in shaping cuticle. Curr Opin Insect Sci
542 19**:** 30-35.
543 Tajiri, R., N. Ogawa, H. Fujiwara and T. Kojima, 2017 Mechanical control of whole body shape by a
544 single cuticular protein obstructor-E in *Drosophila melanogaster*. PLoS Genet 13.
545 Tan, D., X. L. Tong, H. Hu, S. Y. Wu, C. L. Li *et al.*, 2016 Morphological characterization and
546 molecular mapping of an irradiation-induced Speckled mutant in the silkworm, *Bombyx mori*.
547 Insect Mol Biol 25**:** 93-104.
548 Tang, L., J. Liang, Z. Zhan, Z. Xiang and N. He, 2010 Identification of the chitin-binding proteins from
549 the larval proteins of silkworm, *Bombyx mori*. Insect Biochem Mol Biol 40**:** 228-234.
550 True, J. R., 2003 Insect melanism: the molecules matter. Trends Ecol Evol 18**:** 640-647.
551 Van Belleghem, S. M., P. Rastas, A. Papanicolaou, S. H. Martin, C. F. Arias *et al.*, 2017 Complex
552 modular architecture around a simple toolkit of wing pattern genes. Nat Ecol Evol 1.
553 Wang, L.-Y., 2013 Molecular genetic studies on the oily mutants in the silkworm, *Bombyx mori*, pp. 43
554 in *Department of Agricultural and Environmental Biology, Graduate School of Agricultural*
555 *and Life Sciences*. University of Tokyo.
556 Westin, J. E., M. Andersson, M. Lundblad and M. A. Cenci, 2001 Persistent changes in striatal gene
557 expression induced by long-term L-DOPA treatment in a rat model of Parkinson's disease. Eur

bioRxiv preprint first posted online Jun. 27, 2017; doi: http://dx.doi.org/10.1101/155002. The copyright holder for this preprint (which was not peer-reviewed) is the author/funder, who has granted bioRxiv a license to display the preprint in perpetuity. It is made available under a CC-BY-NC-ND 4.0 International license.

J Neurosci 14**:** 1171-1176.

Wilson, K., S. C. Cotter, A. F. Reeson and J. K. Pell, 2001 Melanism and disease resistance in insects. Ecol Lett 4**:** 637-649.

Wittkopp, P. J., and P. Beldade, 2009 Development and evolution of insect pigmentation: genetic mechanisms and the potential consequences of pleiotropy. Semin Cell Dev Biol 20**:** 65-71.

Wittkopp, P. J., S. B. Carroll and A. Kopp, 2003 Evolution in black and white: genetic control of pigment patterns in *Drosophila*. Trends Genet 19**:** 495-504.

Wu, S. Y., X. L. Tong, C. X. Peng, G. Xiong, K. P. Lu *et al.*, 2016 Comparative analysis of the integument transcriptomes of the black dilute mutant and the wild-type silkworm *Bombyx mori*. Sci Rep-Uk 6.

Xiang, Z., 1995 *Genetics and breeding of the silkworm*. Chinese Agriculture Press, Beijing, PR China.

Yoda, S., J. Yamaguchi, K. Mita, K. Yamamoto, Y. Banno *et al.*, 2014 The transcription factor Apontic-like controls diverse colouration pattern in caterpillars. Nat Commun 5**:** 4936.

Acknowledgments

We thank Dr. Tianzhu Xiong, Dr. Yonggang Hu and Ms. Yan Yao for the valuable advices. This work was supported by the Hi-Tech Research and Development 863 Program of China (Grant No. 2013AA102507), the National Natural Science Foundation of China (No. 31302038; 31372379), the Natural Science Foundation Project of ChongQing (CSTC) (No. cstc2013jcyjA80022), China Scholarship Council (201508505020) and Par-Eu Scholars Program (20136666).

Figure legends

Figure 1. Expression of four larval cuticular protein-encoding genes in melanic and non-melanic integuments. A and B represent the gene expressions between the semi-lunar marking (black box) and the non-melanic region (between the semi-lunar marking, red box) in Dazao or Dazao-*stony*, respectively. Scale bar: 2 mm. C. Comparative analysis of gene expressions in the dorsal side of abdominal segments (from the third to the fourth segment, red box) between the p^S and Dazao strains.

bioRxiv preprint first posted online Jun. 27, 2017; doi: http://dx.doi.org/10.1101/155002. The copyright holder for this preprint (which was not peer-reviewed) is the author/funder, who has granted bioRxiv a license to display the preprint in perpetuity. It is made available under a CC-BY-NC-ND 4.0 International license.

587 Scale bar: 1 cm. D. Comparison of gene expressions between the second-instar *al*
588 mutant and the Dazao strain (melanic). The red hashtag symbol indicates the Fig. 1 D
589 we are showing is cited from the previous study of our lab group (Min *et al*. 2016)
590 with modification. Scale bar: 2 mm. *t*-test, n=3; * $p < 0.05$; ** $p < 0.01$; *** $p <$
591 0.001.
592
593 **Figure 2**. Expression of cuticular protein-encoding genes in integuments showing
594 different degree of melanism. A and B display comparisons of degree of melanism
595 and cuticular protein-encoding gene expression levels among four strains with mutant
596 alleles at the *p* locus. Scale bar: 1 cm. Ratios represent the ratios of gene expression
597 levels between two strains. Symbols (−, +, ++, and +++) represent the increment of
598 the degree of melanism. Star represents the melanin-associated cuticular
599 protein-encoding genes. *t*-test, n=3; * $p < 0.05$; ** $p < 0.01$.
600
601 Figure 3. Segregation patterns of the phenotypes of progenies from different crosses
602 of melanic mutant strains and the *stony* strain. In the segregated progenies, the first
603 item in the list (B,N), (B,st), (S,N), (S,st), (M,N), (M,st), (N,N) and (N,st) represents
604 p^B-, p^S- p^M- and Normal color patterns, respectively. The second item indicates body
605 shape features marked with non-*stony* type (N) and the *stony* type (st). It is
606 noteworthy that in (S, st-am+) and (M, st-am+), the second item represents the
607 ambiguous *stony* body shape. The size of "+" symbol represents the corresponding
608 degree of the ambiguous *stony* body shape. Superscript "T"s represent theoretical

bioRxiv preprint first posted online Jun. 27, 2017; doi: http://dx.doi.org/10.1101/155002. The copyright holder for this preprint (which was not peer-reviewed) is the author/funder, who has granted bioRxiv a license to display the preprint in perpetuity. It is made available under a CC-BY-NC-ND 4.0 International license.

609 values. Superscript "A"s represent actual values. Backslashes indicates that a value
610 was not obtained. Chi-squared test, * $p < 0.05$; ** $p < 0.01$.

611

612 Figure 4. Association analysis of the genotypes, phenotypes and gene expression
613 levels in segregated progenies from different crosses. A. Correlation analysis between
614 the genotypes and phenotypes in self-crossed or backcrossed progenies. Scale bar: 1
615 cm. White and red stars represent polymorphic bands at the $+^{p}$ and p^{X} loci (X = *B*, *S* or
616 *M*), respectively. Red and white hash-tag represent polymorphic bands at the *st* and $+^{st}$
617 locus, respectively. Solid and dotted red arrows indicate the relative degree of bulging
618 (solid > dotted), respectively. Slashes show the genotypes within one phenotypic
619 category. The thickness of the slash represents the proportion of the corresponding
620 genotypes. Dotted backslashes indicate that the number of individuals with the
621 corresponding genotype is quite low. B. Ratios of the length of internodes and
622 intersegmental folds in the second, third, and fourth abdominal segments of
623 individuals with different genotypes (showing melanic body color) in the self-crossed
624 or backcrossed progenies. n≥3, *t*-test, ** $p < 0.01$. C. Gene expression analysis of
625 cuticular protein-encoding genes in homogeneous and heterogeneous individuals at
626 the *p* locus from self-crossed progenies of p^{S} × *stony*, and p^{M} × *stony* under the
627 condition that the cuticle was melanic and the genotype was homozygous recessive at
628 *st* locus. n = 3, *t* – test, * $p < 0.05$; ** $p \leq 0.01$.

629

630 Figure 5. Effect of melanin precursors (top left: in cells) and BH_4 (top right: in *vivo*)

bioRxiv preprint first posted online Jun. 27, 2017; doi: http://dx.doi.org/10.1101/155002. The copyright holder for this preprint (which was not peer-reviewed) is the author/funder, who has granted bioRxiv a license to display the preprint in perpetuity. It is made available under a CC-BY-NC-ND 4.0 International license.

631 treatments on the expression of cuticular protein-enconding genes (*t*-test; n = 3, * $p <$
632 0.05; ** $p < 0.01$), and variations of gene expression levels in larval cuticle treated
633 with the inhibitor DAHP (bottom). n = 3, *t*-test, ** $p < 0.01$.
634
635 **Figure 6.** Schematic overview of the effect of melanin precursors on the expressions
636 of cuticular protein-encoding genes. Black solid circles represent the melanin.
637 Triangles represent the BmLcps with similar expression patterns and functions. Solid
638 and hollow triangles represent the normal and defective functions, respectively.
639 Brown rhombi represent other components (such as chitin) in the cuticle. Solid
640 double-headed arrow indicates the probable interaction between the endocuticular
641 proteins and other components. Combination of the single-headed arrow and the letter
642 'R' indicate the repair of the potential defects through functional complementary.
643 Purple arrows show the direction in which the melanin precursors or cuticular proteins
644 flow from the haemolymph to the epidermal cells as well as from the epidermal cells
645 to the cuticle. Red arrows indicate the increased contents of melanin precursors or the
646 up-regulation of cuticular protein-encoding genes. Purple polyline arrows indicate
647 melanism-promoting factors produced by other genetic instructions. Double dovetail
648 arrows indicate the effect of melanin precursors on cuticular protein-encoding genes.
649 The question mark indicates that the details of induction (directly or indirectly) are
650 unclear.
651

Figure 1

bioRxiv preprint first posted online Jun. 27, 2017; doi: http://dx.doi.org/10.1101/155002. The copyright holder for this preprint (which was not peer-reviewed) is the author/funder, who has granted bioRxiv a license to display the preprint in perpetuity. It is made available under a CC-BY-NC-ND 4.0 International license.

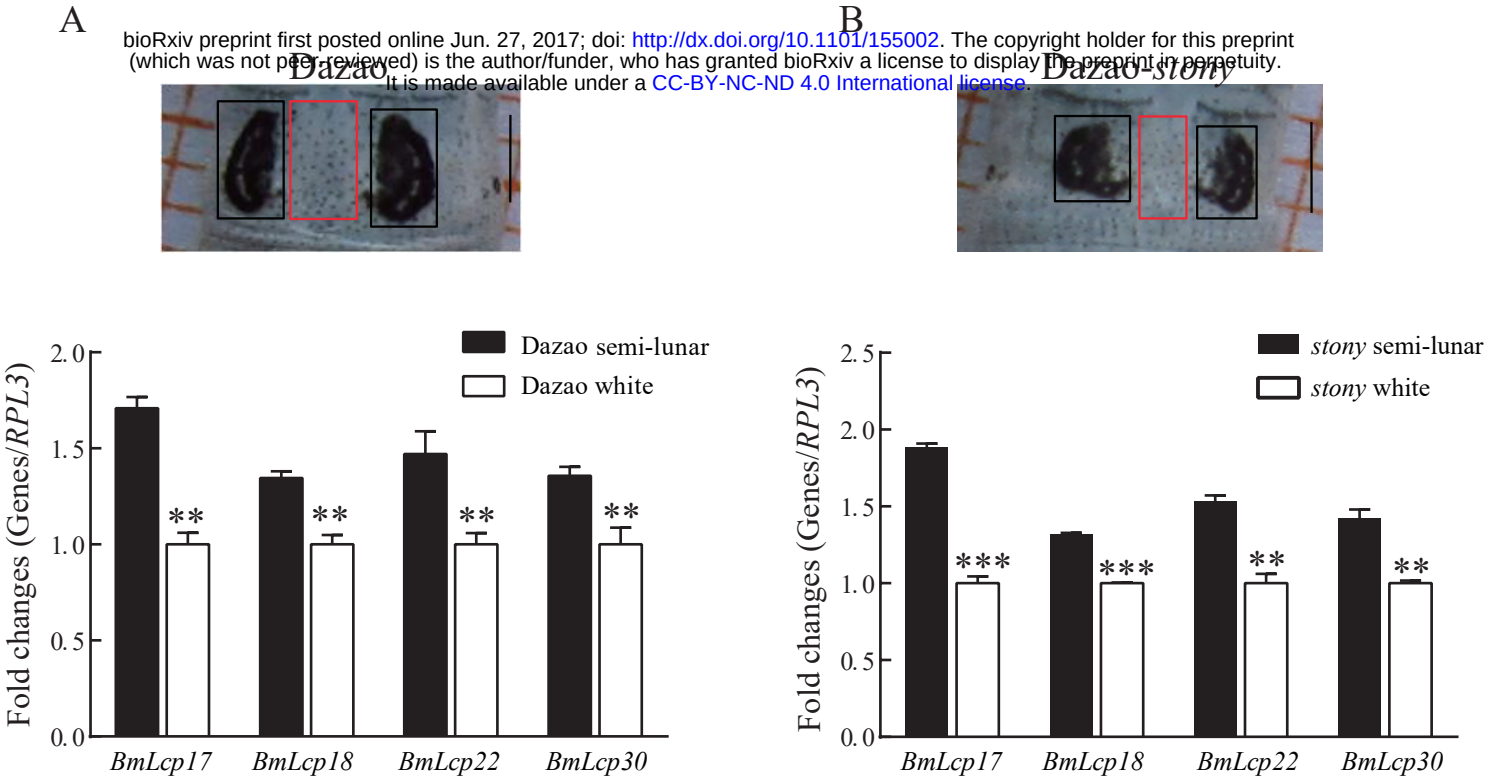

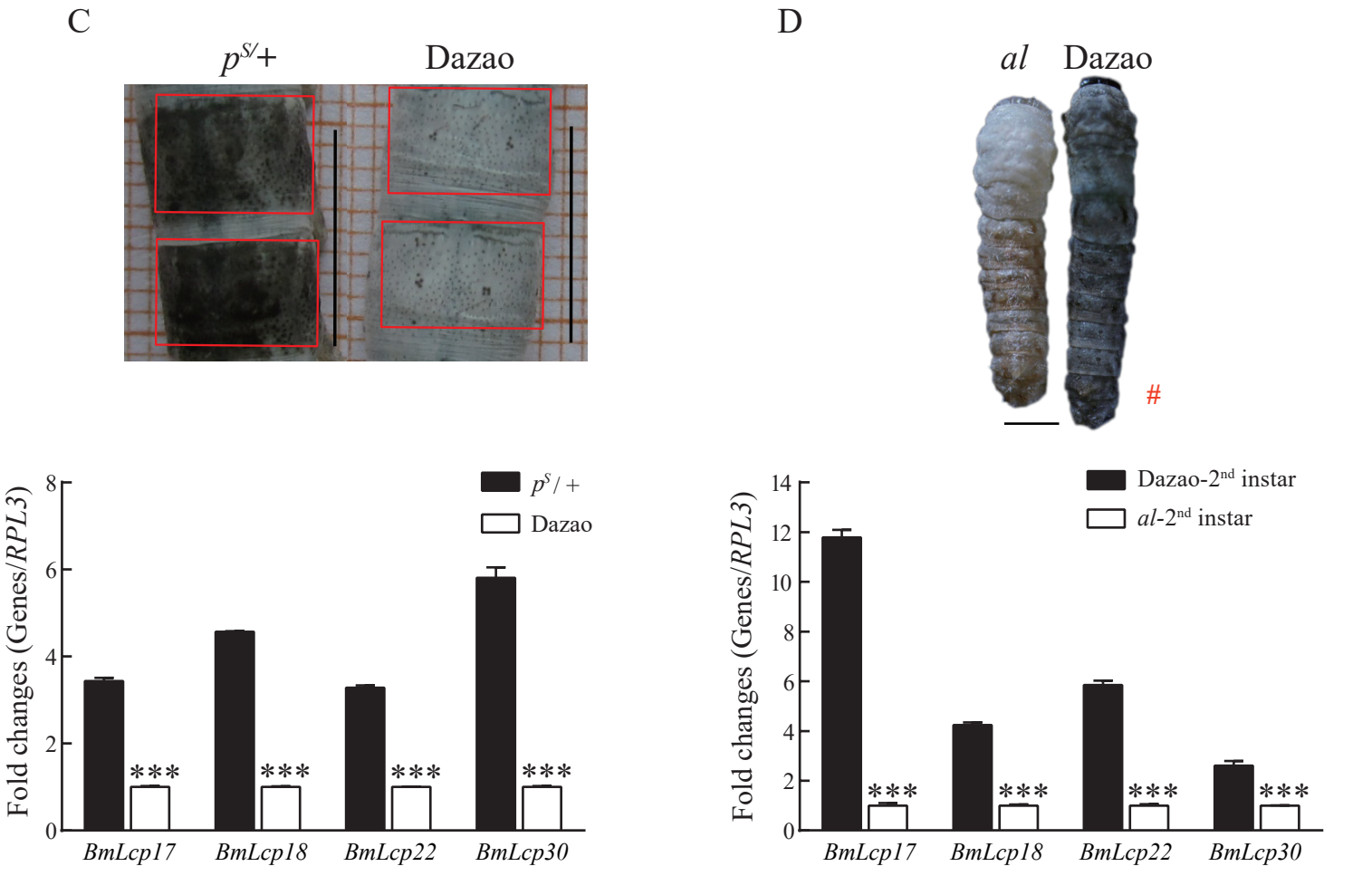

Figure 2

bioRxiv preprint first posted online Jun. 27, 2017; doi: http://dx.doi.org/10.1101/155002. The copyright holder for this preprint (which was not peer-reviewed) is the author/funder, who has granted bioRxiv a license to display the preprint in perpetuity. It is made available under a CC-BY-NC-ND 4.0 International license.

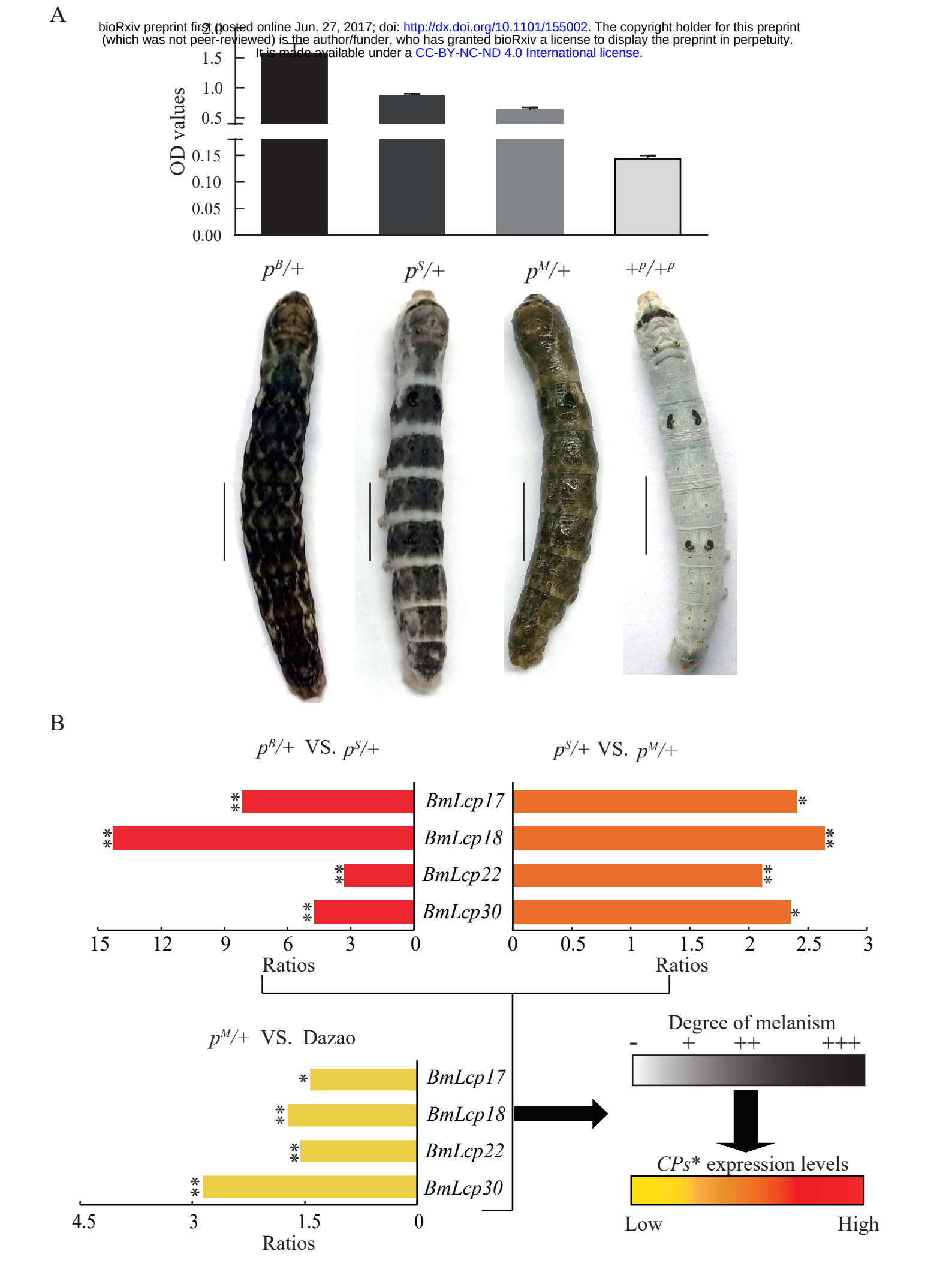

Figure 3

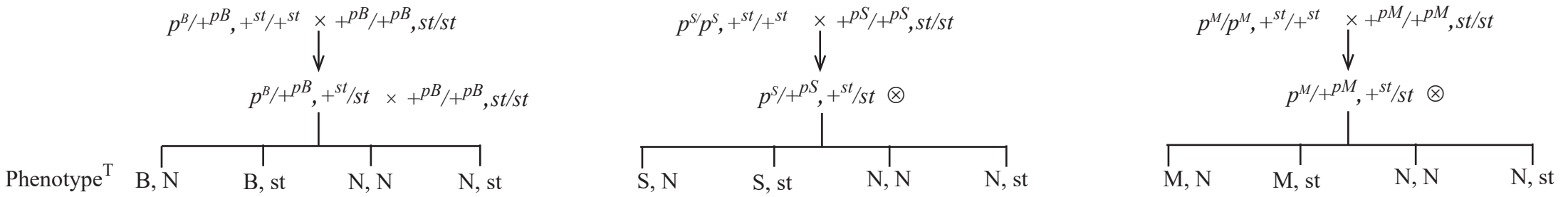

Phenotype^T	B, N	B, st	N, N	N, st	S, N	S, st	N, N	N, st	M, N	M, st	N, N	N, st
Ratios^T	1	1	1	1	9	3	3	1	9	3	3	1
Genotype^T	$p^B/+^{pB}$, $+^{st}/st$	$p^B/+^{pB}$, st/st	$+^{pB}/+^{pB}$, $+^{st}/st$	$+^{pB}/+^{pB}$, st/st	$p^S/_$, $+^{st}/_$	$p^S/_$, st/st	$+^{pS}/+^{pS}$, $+^{st}/_$	$+^{pS}/+^{pS}$, st/st	$p^M/_$, $+^{st}/_$	$p^M/_$, st/st	$+^{pM}/+^{pM}$, $+^{st}/_$	$+^{pM}/+^{pM}$, st/st
Phenotype^A	B, N	B, st	N, N	N, st	S, N	S, st	S, st-am+	N, N	N, st	M, N	M, st	M, st-am+	N, N	N, st
Ratios^A	2.1	\	1	0.9	10.29	\	1.74	2.95	1	10.07	\	1.86	3.07	1
Numbers^A	290**	0**	138	125	213*	0**	36**	61	21	275*	0**	51**	84	27

Figure 4

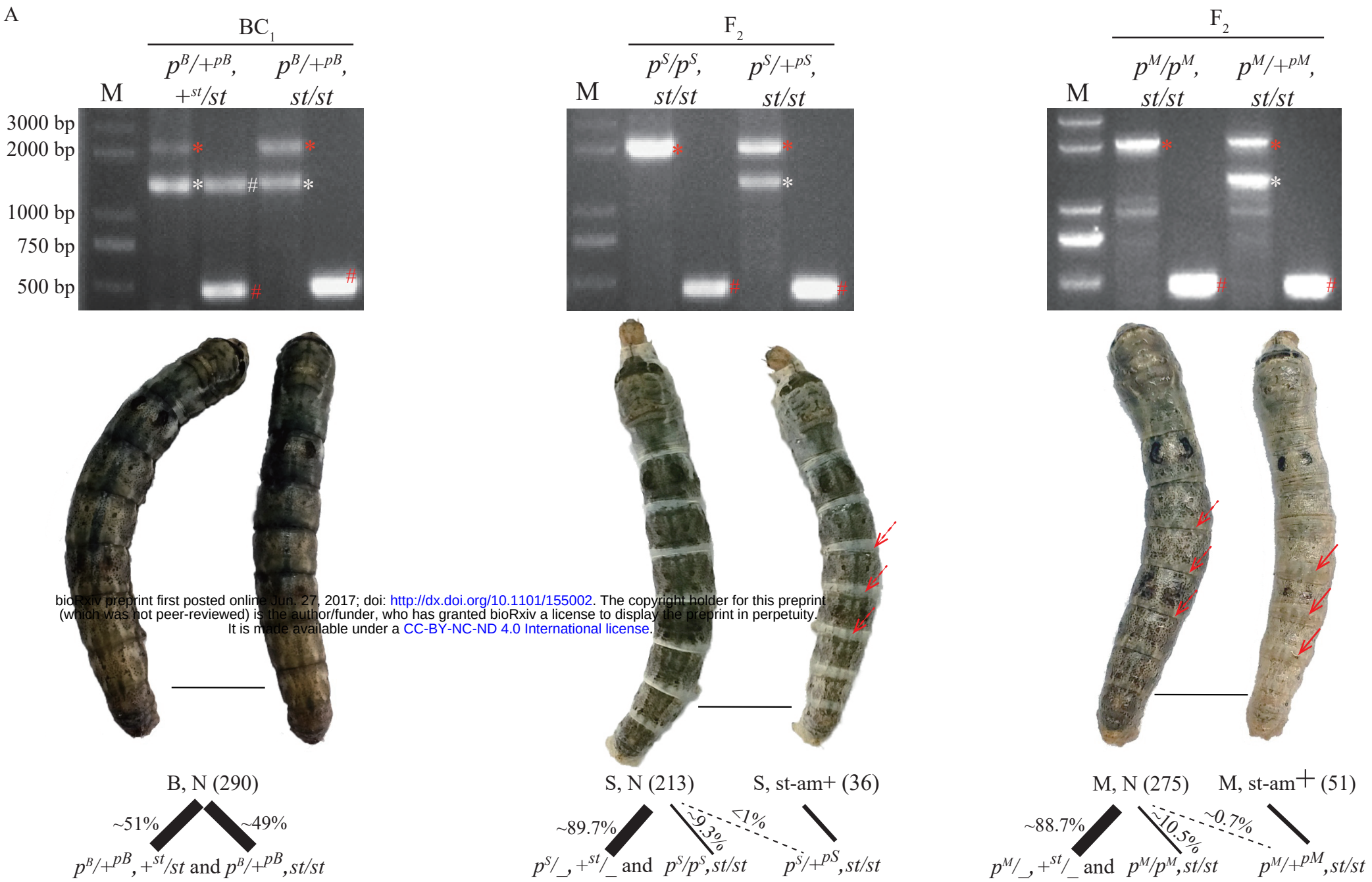

bioRxiv preprint first posted online Jun. 27, 2017; doi: http://dx.doi.org/10.1101/155002. The copyright holder for this preprint (which was not peer-reviewed) is the author/funder, who has granted bioRxiv a license to display the preprint in perpetuity. It is made available under a CC-BY-NC-ND 4.0 International license.

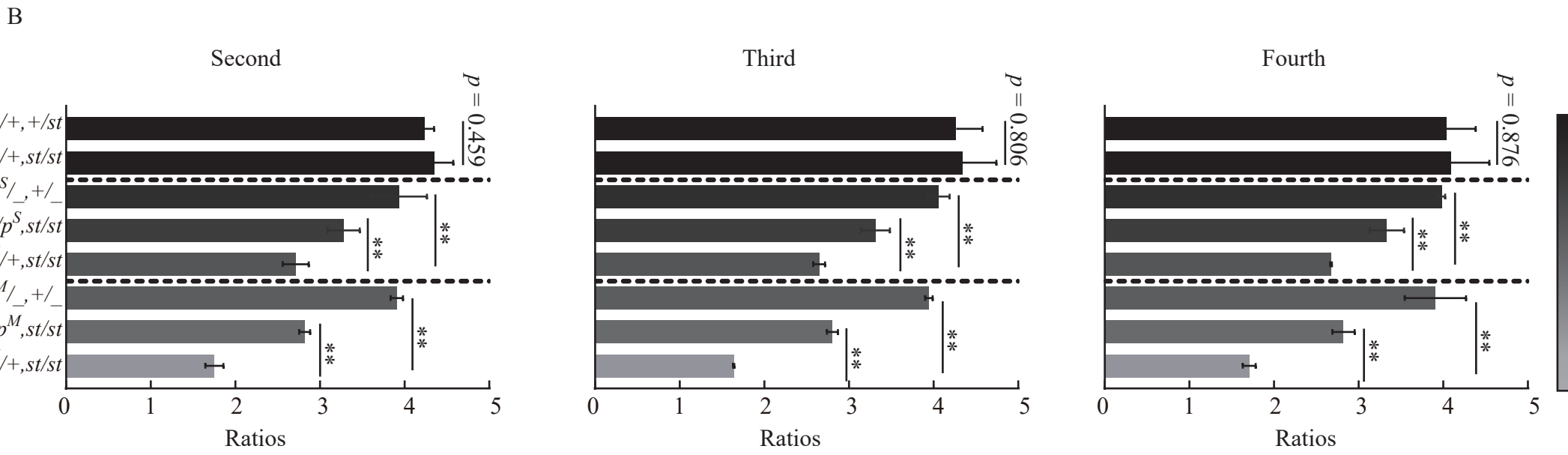

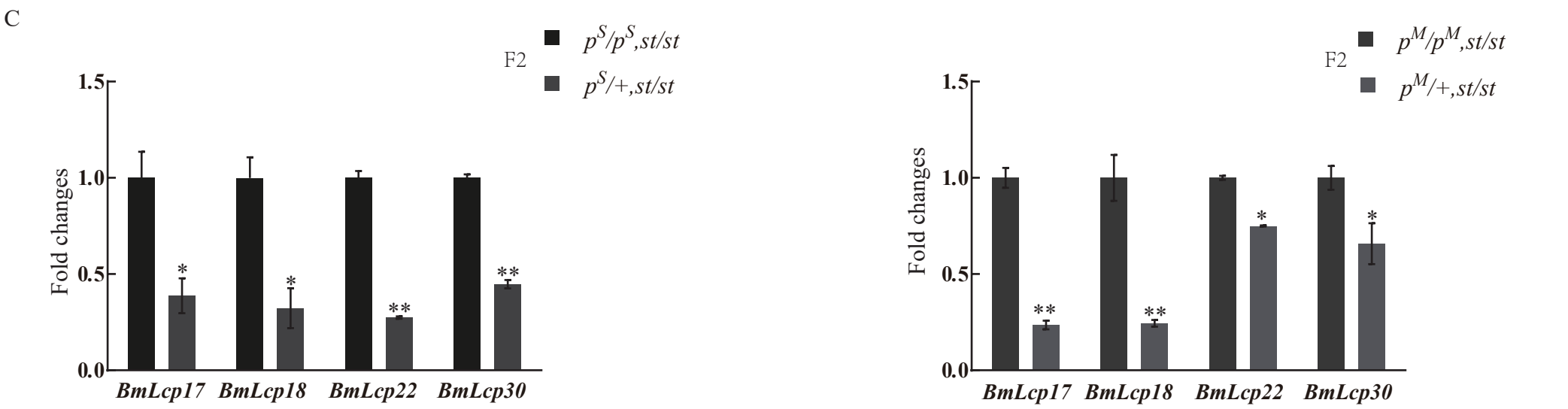

Figure 5

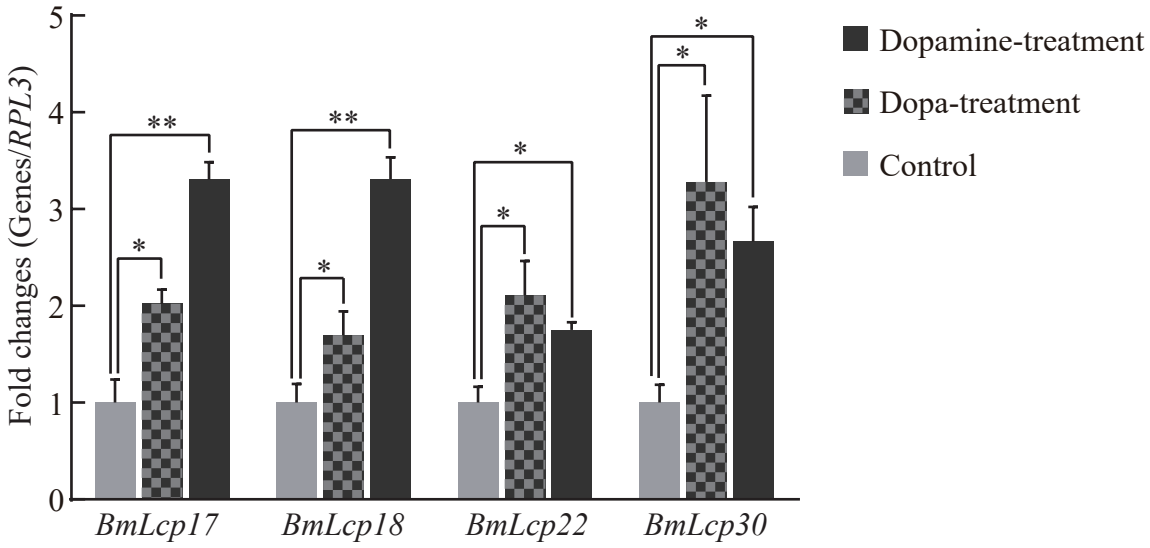

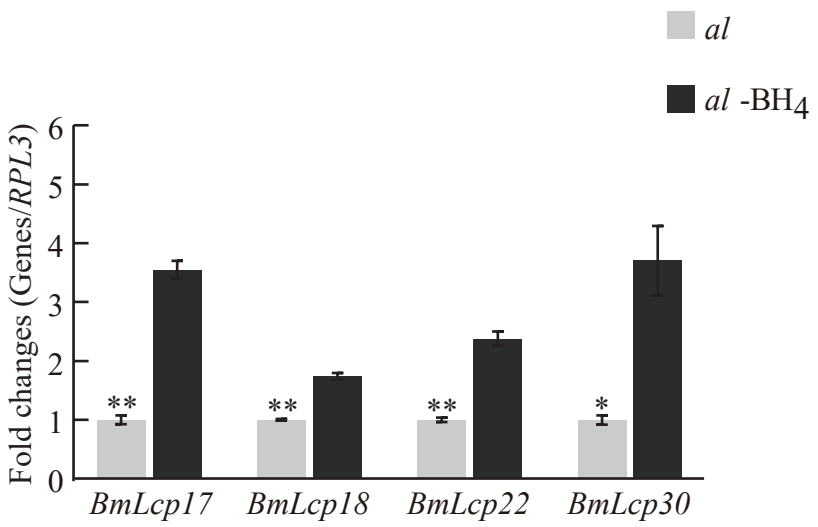

bioRxiv preprint first posted online Jun. 27, 2017; doi: http://dx.doi.org/10.1101/155002. The copyright holder for this preprint (which was not peer-reviewed) is the author/funder, who has granted bioRxiv a license to display the preprint in perpetuity. It is made available under a CC-BY-NC-ND 4.0 International license.

Contents of melanin precursors

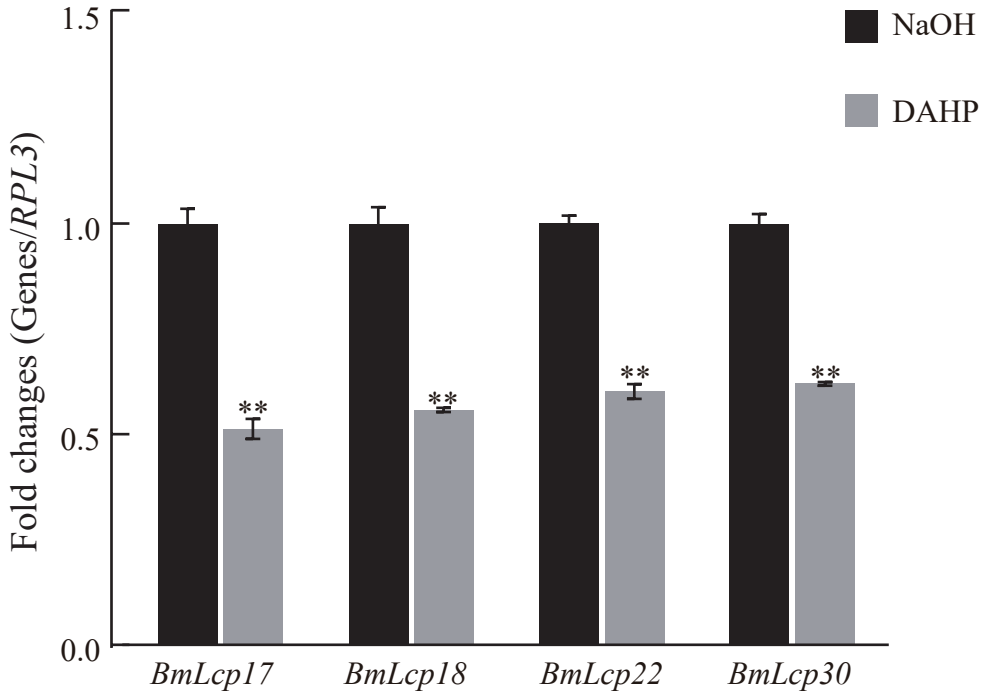

Figure 6
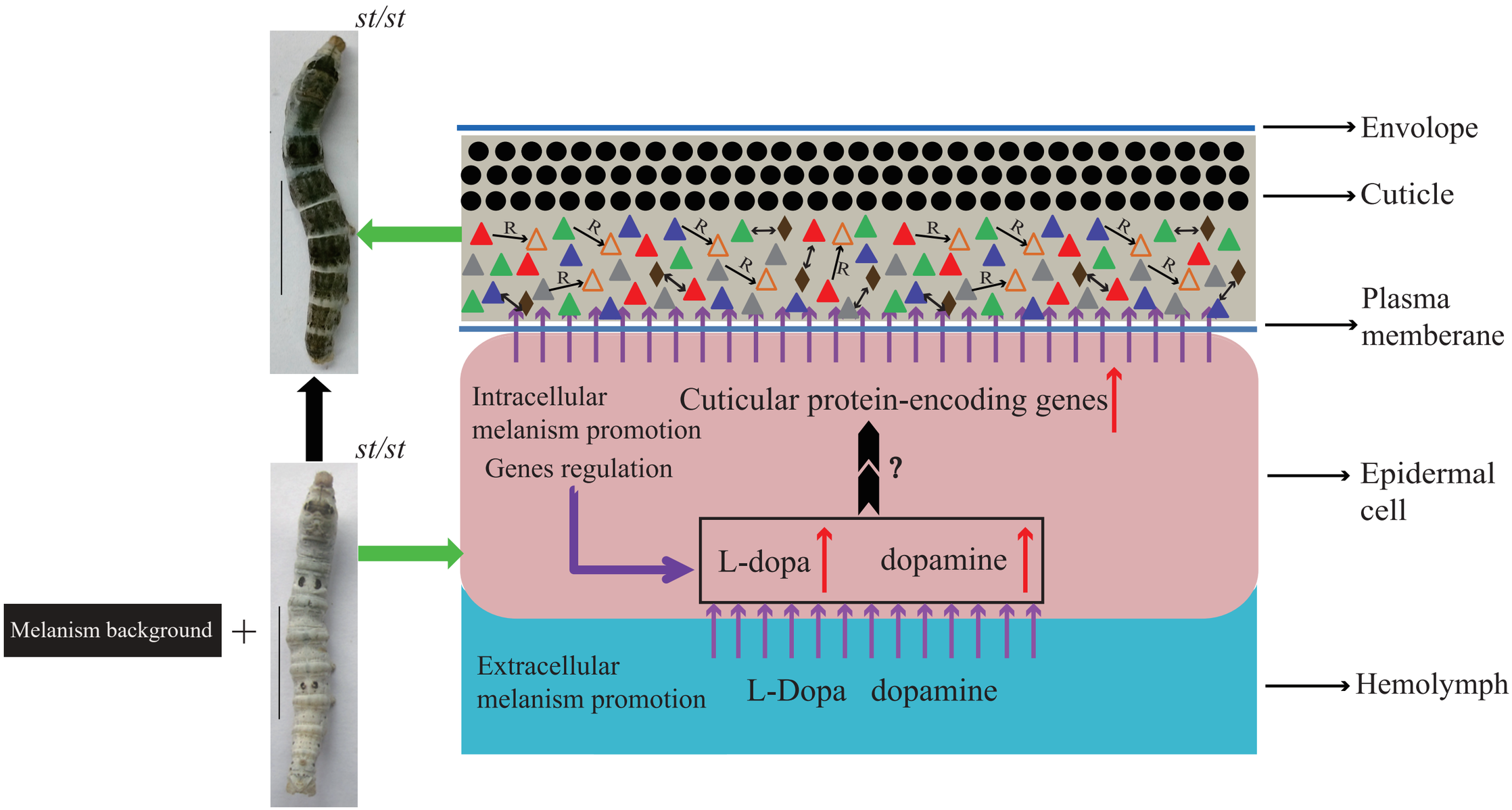
bioRxiv preprint first posted online Jun. 27, 2017; doi: http://dx.doi.org/10.1101/155002. The copyright holder for this preprint (which was not peer-reviewed) is the author/funder, who has granted bioRxiv a license to display the preprint in perpetuity. It is made available under a CC-BY-NC-ND 4.0 International license.